Confinement mechanism in the Field Correlator Method

Yu.A.Simonov, ITEP, Moscow

Talk at the 2010 – Slavnov Feast 20-23 January 2010

Contents:

1. Introduction: Mass scales in QCD.
2. Perturbative and Nonperturbative.
3. Basics of Field Correlator Method.
4. Explaining Meson and Glueball scales via string tension.
5. Deconfinement. Explaining T_c via Gluon condensate.
6. Field Correlators via Gluelumps and Gluelumps via Field correlators.
7. Check of selfconsistency at small and large distances. Λ_{QCD} via string tension.
8. Conclusions.

1. Introduction: Mass scales in QCD

QCD is the selfconsistent quantum field theory which is defined by the QCD Lagrangian, not containing any dimensionful parameters (except for quark masses), and one needs one additional mass scale ($\mathcal{M}$) to fix the theory.

In gluodynamics one can choose $\Lambda_{QCD} \approx 0.3$ GeV or string tension $\sigma = 0.18$ GeV^2. They should be connected to one scale $\mathcal{M}$.

But there are other scales in QCD, which are very different

Glueball mass: $m_G = O(2\ \mathrm{Gev})$.

Deconfinement temperature $T_c = 0.27$ GeV$\div 0.17$ GeV for $n_f = 0 - 2$.

Gluonic condensate $G_2 = \frac{\alpha_s}{\pi}\langle F_{\mu\nu}F_{\mu\nu}\rangle = 0.012 \pm 0.006\ \mathrm{GeV}^4$.

$$f_\pi = 0.093GeV, \quad m_\pi = 0.14GeV$$

We aim at explaining all different scales in term of the only one, say $\mathcal{M}$. This is done in the framework of Field Correlator method (FCM).

Talk is based on many papers including recent V.I.Shevchenko, Yu.A.Simonov, arXiv:0902.1405.

2. Perturbative and Nonperturbative

The very concept of finite G_2 introduced by SVZ implies possibility of separation of Perturbative and Nonperturbative contributions in QCD. On general grounds for every physical amplitude of dimension $m^2 = L^{-2}$ the finite sum of Perturbative terms yields $\sim L^{-2} f\left(ln\frac{1}{L\Lambda_{QCD}}\right)$, while Nonperturbative $\sim \mathcal{M}^2$. In principle there can be mixed terms $O\left(\frac{\mathcal{M}}{L},\ L\mathcal{M}^3, ..\right)$.
We shall prove that for Field correlator one can write $(x \to y)$

$$\frac{g^2}{4\pi^2}\langle trF_{\mu\nu}(x)\Phi(x,y)F_{\mu\nu}(y)\Phi(y,x)\rangle =$$

$$= Pert.\left(O\left(\frac{ln(x-y)}{(x-y)^4}\right)\right) + G_2 + ...$$

Infinite Pert. series are not defined due to IR renormalons, and perturbation theory in QCD has sense when background vacuum fields are taken into account. Confining background fields eliminate IR renormalons and define IR stable perturbative theory (Yu.S. 1993)

$$\alpha_s(q) = \frac{4\pi\left(1 + O\left(\frac{lnln}{ln}\right)\right)}{\beta ln\left(\frac{q^2+M_b^2}{\Lambda^2_{QCD}}\right)}.$$

The new scale $M_b \cong 1$ GeV is expressed via σ and is related to the hybrid masses.

Thus background Perturbation Theory with nonperturbative background is a selfconsistent theory with a Borel summable series.

Note, that Landau ghost is absent when NP vacuum is taken into account – this justifies the Analytic Pert. Theory (D.V.Shirkov et al.)

3. Basics of Field Correlator Method

As will be shown below, Green's function of any white system is proportional to the path integral of the Wilson loop.

For $q\bar{q}, G_{q\bar{q}} \sim \int (Dz)\langle trW(C)\rangle$... Therefore Wilson loop defines the dynamics (pert. and nonpert.) of light and heavy quarks.

Building blocks: Wegner-Wilson loops

$$W(C) = \mathrm{P}\exp ig \oint\limits_C A^a_\mu(z) t^a dz_\mu \tag{1}$$

Parallel transporter

$$\Phi(x;y) = \mathrm{P}\exp ig \int\limits_x^y A^a_\mu(z) t^a dz_\mu \tag{2}$$

Field strength

$$F_{\mu\nu}(x) = \partial_\mu A_\nu - \partial_\nu A_\mu - ig[A_\mu, A_\nu]$$

Field correlators

$$D^{(n)}_{\mu_1\nu_1...\mu_n\nu_n}(x_1, ..., x_n) =$$

$$= \left(\frac{g}{\sqrt{N_c}}\right)^n \langle \mathrm{Tr}\, F_{\mu_1\nu_1}(x_1)\Phi(x_1, x_2)F_{\mu_2\nu_2}(x_2)...F_{\mu_n\nu_n}(x_n)\Phi(x_n, x_1)\rangle \quad (3)$$

Nonabelian Stokes Theorem and Cluster Expansion

The basic element of Nonperturbative QCD – the correlator $D^{(2)}_{\mu\nu\rho\sigma}$.

$$\Delta^{(2)}[S] = \frac{1}{2}\int\limits_S d\sigma_{\mu\nu}(z_1)\int\limits_S d\sigma_{\rho\sigma}(z_2) D^{(2)}_{\mu\nu\rho\sigma}(z_1,z_2) \tag{4}$$

$$\Delta^{(2)}[S] = \sigma S$$

Gauge-invariant Field Correlators $D^{(2)}$ define the most part of nonperturbative (and perturbative $O(\alpha_s)$) dynamics

$$D^{(2)}_{\mu\nu\rho\sigma}(z) = \frac{g^2}{N_c}\langle \mathrm{Tr}\, F_{\mu\nu}(x)\Phi F_{\rho\sigma}(y)\Phi\rangle \tag{5}$$

Two basic scalars: D and D_1 (Dosch+ Yu.S., ('88)).

$$D^{(2)}_{\mu\nu\rho\sigma}(z) = (\delta_{\mu\rho}\delta_{\nu\sigma} - \delta_{\mu\sigma}\delta_{\nu\rho})D(z) + \\ +\frac{1}{2}\left(\frac{\partial}{\partial z_\mu}(z_\rho\delta_{\nu\sigma} - z_\sigma\delta_{\nu\rho}) - \frac{\partial}{\partial z_\nu}(z_\rho\delta_{\mu\sigma} - z_\sigma\delta_{\mu\rho})\right) D_1(z) \qquad (6)$$

$D(x)$ is purely nonperturbative (pert. cancel-Shevchenko+Yu.S.'98).

Important: Dominance of Gaussian correlator $D^{(2)}(z) \to$ the QCD vacuum is almost $(> 95\%)$ Gaussian (Bali '99, Shevchenko and Yu.S.'00).Check: Casimir scaling – $\Delta^{(2)} \sim C_2$, hence all $Q\bar{Q}$ potentials in different representations (j) are proportional to $C_2(j)$. Odd n correlations vanish on flat surfaces).

$$\Delta^{(2)}[S] \gg \sum_{n=3}^{\infty} \Delta^{(n)}[S] \qquad (7)$$

If (connected) average $D^{(n)}(x_1 - x_2, ...) \sim \exp(-\frac{|x_i - x_j|}{\lambda})$ for large $|x_i - x_j|$, then

$$\frac{\Delta^{(n+2)}[S]}{\Delta^{(n)}[S]} \approx \lambda^4 \langle F^2 \rangle \approx \sigma \lambda^2$$

It will be shown, that $\lambda \sim 0.1$fm, and expansion parameter is $\sigma\lambda^2 \sim 0.05$. Therefore all $\Delta^{(n)}$ with $n > 2$ contribute few percent.

$$\langle \mathrm{Tr}\, W(C) \rangle = \left\langle \mathrm{Tr}\, \mathcal{P} \exp ig \int\limits_S \Phi F_{\mu\nu}(z) \Phi d\sigma_{\mu\nu}(z) \right\rangle =$$

$$= \exp \sum_{n=2}^{\infty} (i)^n \Delta^{(n)}[S] = \exp(-V(R)T) \qquad (8)$$

Static potentials from rectangular WW loop $(R \times T)$,

$$\langle trW(C)\langle = \exp(-TV(R))$$

$$V(R) = V_D(R) + V_1(R)$$

$$V_D(R) = 2\int_0^R (R-\rho)d\rho \int_0^\infty d\nu D(\sqrt{\rho^2+\nu^2}), \tag{9}$$

$$V_1(R) = \int_0^R \rho d\rho \int_0^\infty d\nu D_1(\sqrt{\rho^2+\nu^2}). \tag{10}$$

Check of Gaussian vacuum QCD

Casimir scaling

$V_D, V_1 \sim C_2(d)$ for Gaussian vacuum, $d =$ fund, adj. etc.

Polyakov lines – basic dynamics for deconfined state

$L(d) = \exp\left(-\frac{V_1(\infty)}{2T}\right), T$ – temperature

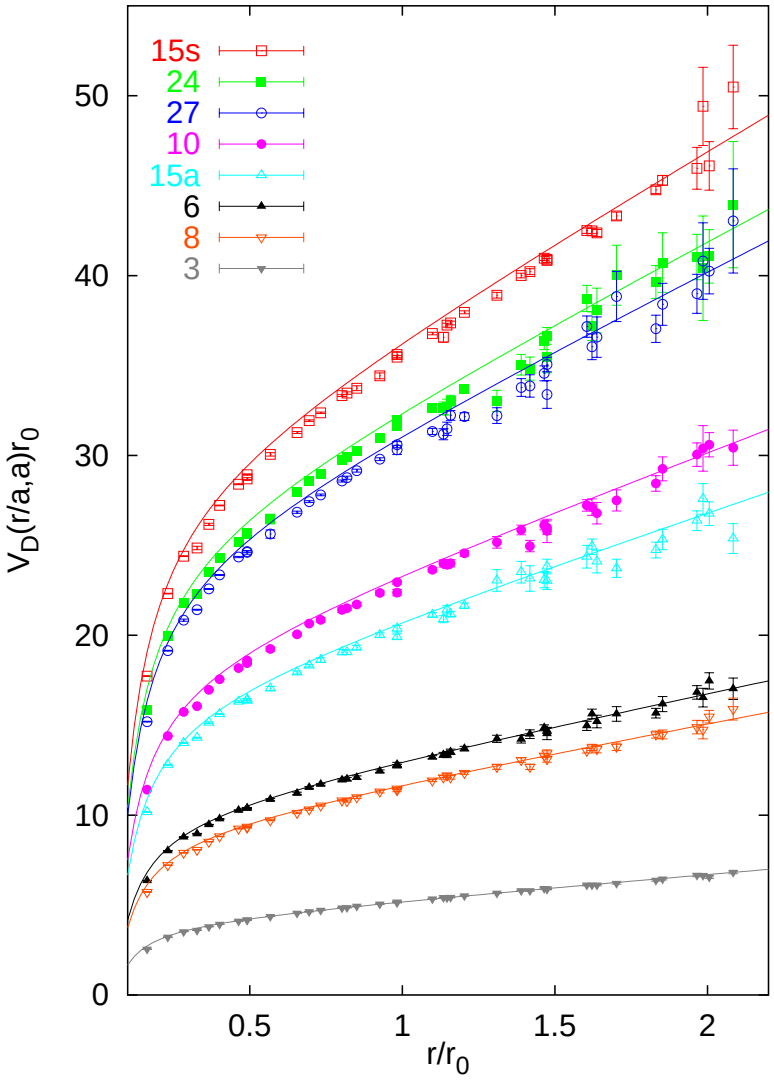

Figure 1:

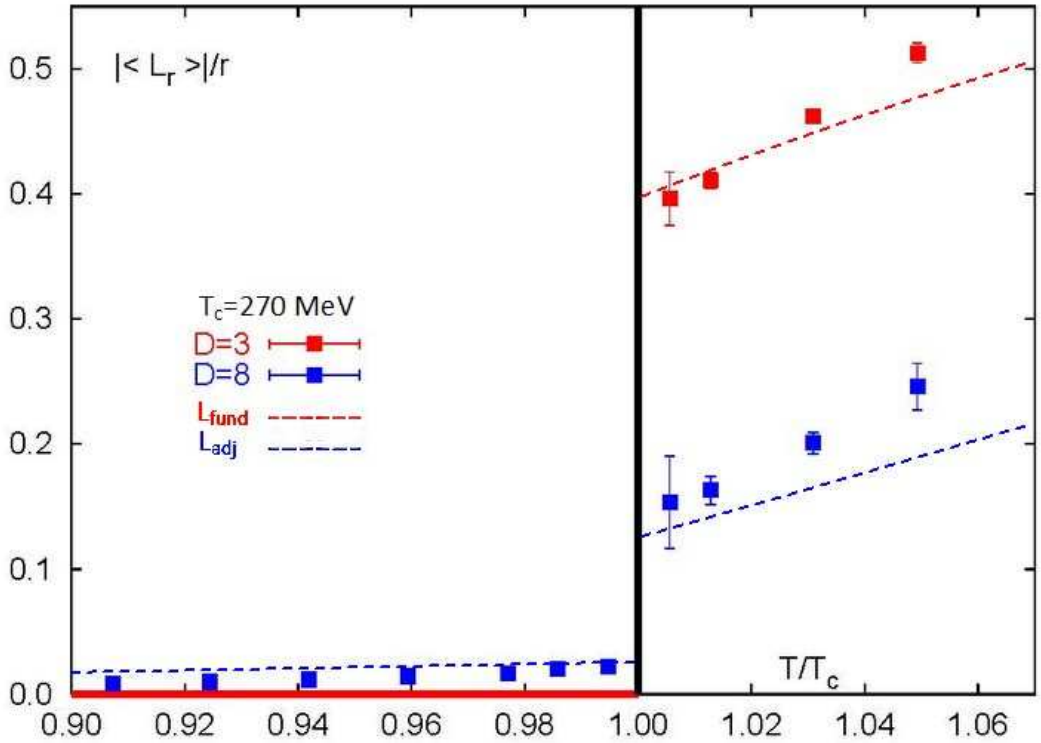

Figure 2: Shown on the figure are curves of L_{adj} (blue dashed) and L_{fund} (red dashed) compared to the ones taken from [**?**]. In the $T < T_c$ region the $M(\bar{\alpha}_s = 0.195) = 0.982$ GeV gluelump mass was used. In the deconfinement region the fit (**??**) was used with $T_c = 270$ MeV for L_{fund} and the Casimir scaled value for L_{adj}.

Casimir scaling and topcharges

Topological charges imply coherence and hence are opposite to stochastic (Gaussian) vacuum. Coherence means large role of higher cumulants – no Casimir scaling.

Instanton gas violates $\frac{V(adj)}{V(fund)}$ by $\sim 20\%$

Center vortices violate by $\sim 30\%$.

Actually cumulant expansion diverges for the gas of topcharges, since expansion parameter reduces to elementary flux $= g \int F_{\mu\nu} \Delta\sigma_{\mu\nu} = 2\pi$ for instantons, π for magnetic monopoles.

Casimir scaling implies suppression of topcharges in the QCD vacuum (Shevchenko and Yu. S.)

From lattice and analytic data

$$D(x) \sim \exp(-|x|/\lambda),$$

Important feature of QCD vacuum! Vacuum correlator length λ
Campostrini, Di Giacomo, Olejnik ('86).
Di Giacomo et al. $\lambda \approx 0.2 \div 0.3$ fm
Bali, Brambilla, Vairo $\lambda \lesssim 0.2$ fm
Dosch et al. $\lambda \lesssim 0.2$ fm
Yu.S. $\lambda \approx 0.15$ fm.

Recently $D(x), D_1(x)$ were computed on lattice (Koma and Koma) in evaluating spin-dependent potentials. Results are compatible with $\lambda \lesssim 0.1$ fm.

$HP(1)$ projection of $SU(2)$ gluodynamics. V.Orlovsky, V.Shevchenko ('09)

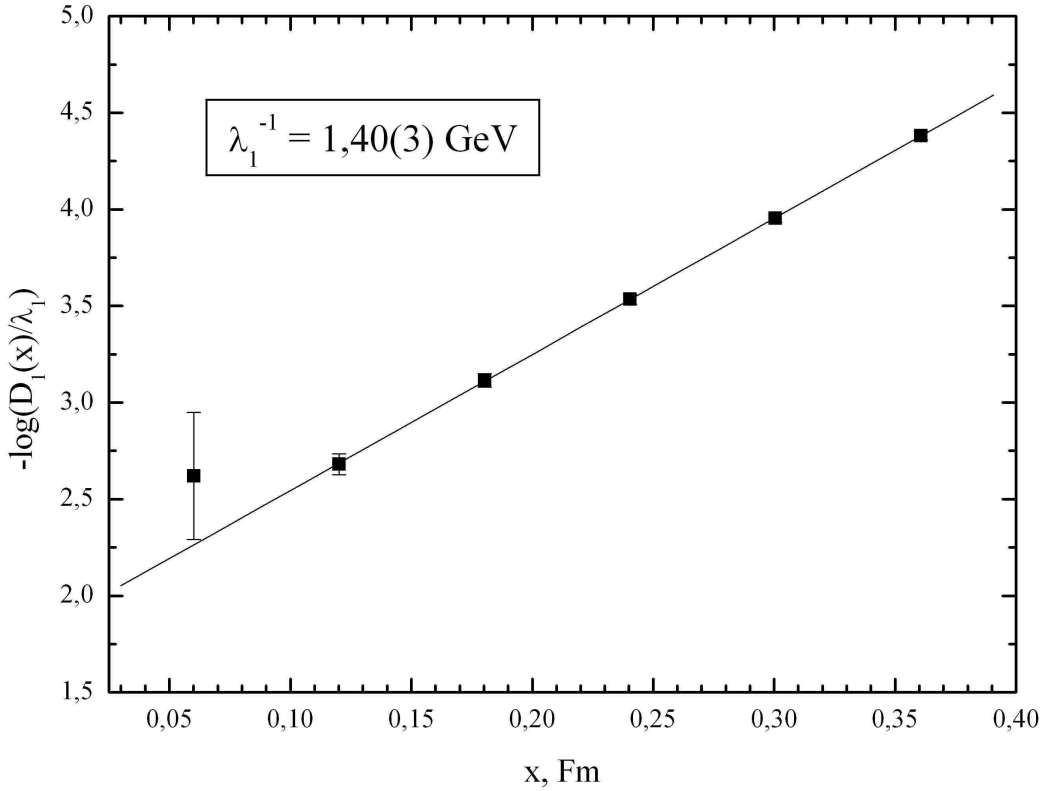

Figure 3: Function $\log D_1(x)$ (conventional units) from the measurements of two point correlators (9)

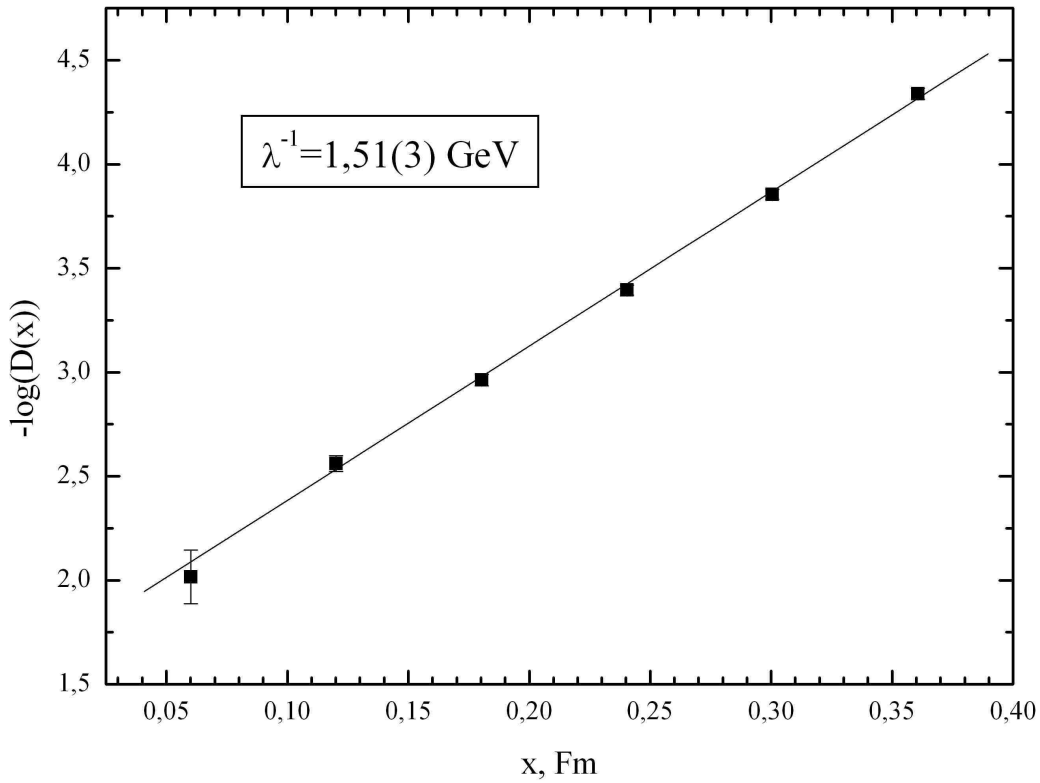

Figure 4: Function $\log D(x)$ (conventional units) from the measurements of two point correlators (9)

D ensures confinement

$$V_D(R) = \sigma R + \mathcal{O}(R^0) \quad ; \quad \sigma = \frac{1}{2}\int d^2 z D(z), R \to \infty \tag{11}$$

$$V_D(R) = cR^2 + O(R^4), \quad R \lesssim \lambda \tag{12}$$

D_1 contains all (but not confinement), $V_1(R) = V_1^{(pert)} + V_1^{(nonpert)}$

$$V_1^{(nonpert)}(R \to \infty) = const \sim 0.5 GeV \tag{13}$$

V_1 supports bound states $Q\bar{Q}$ in quark-gluon plasma (Yu.S.'91, '05)

$$V_1^{(pert)} = -\frac{4(\alpha_s + O(\alpha_s^2))}{3R}. \tag{14}$$

Eichten-Feinberg formula spin-dependent potentials in heavy quarkonia

$$V_{SD}(r) = \left(\frac{\boldsymbol{\sigma}_1 \mathbf{L}}{4m_1^2 r}\frac{\boldsymbol{\sigma}_2 \mathbf{L}}{4m_2^2 r}\right)[V_0'(r) + V_1'(r)] + \frac{(\boldsymbol{\sigma}_1 + \boldsymbol{\sigma}_2)\mathbf{L}}{2m_1 m_2 r} V_2'(r)$$

$$+ \frac{3(\boldsymbol{\sigma}_1 \mathbf{n})(\boldsymbol{\sigma}_2 \mathbf{n}) - \boldsymbol{\sigma}_1 \boldsymbol{\sigma}_2}{12 m_1 m_2} V_3(r) + \frac{\boldsymbol{\sigma}_1 \boldsymbol{\sigma}_2}{12 m_1 m_2} V_4(r)$$

Potentials in the FCM

$$V_0'(r) = 2\int_0^\infty d\nu \int_0^r d\lambda D^E(\lambda,\nu) + r\int_0^\infty d\nu D_1^E(r,\nu)$$

$$V_1'(r) = -2\int_0^\infty d\nu \int_0^r d\lambda \left(1-\frac{\lambda}{r}\right) D^H(\lambda,\nu)$$

$$V_2'(r) = \frac{2}{r}\int_0^\infty d\nu \int_0^r \lambda d\lambda D^H(\lambda,\nu) + r\int_0^\infty d\nu D_1^H(r,\nu)$$

$$V_3(r) = -2r^2\frac{\partial}{\partial r^2}\int_0^\infty d\nu D_1^H(r,\nu)$$

$$V_4(r) = 6\int_0^\infty d\nu \left[D^H(r,\nu) + \left[1+\frac{2}{3}r^2\frac{\partial}{\partial \nu^2}\right] D_1^H(r,\nu)\right]$$

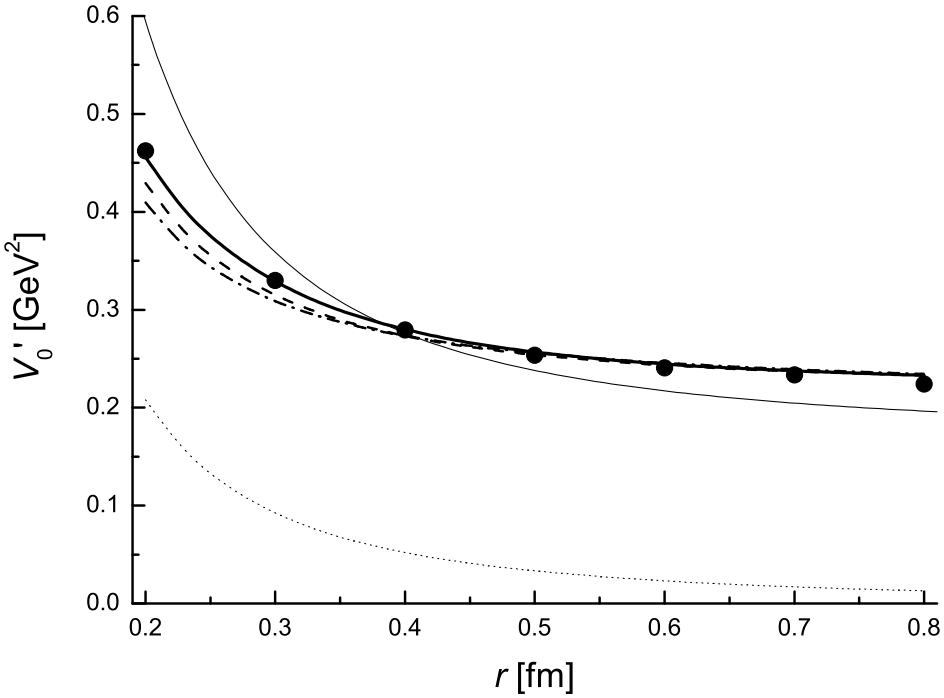

Figure 5: The profile of the $V_0'(r)$ for the set 1 (dash-dotted line), set 2 (dashed line), set 3 (fat solid line), set 4 (doted line), and set 5 (thin solid line). Lattice data are given by dots.

4. Expaining meson and glueball scales via string tension

Quark Green's function (Euclidean)

$$S_q(x,y) = (m + \hat{D})^{-1} = (m - \hat{D}) \int_0^\infty ds (Dz)_{xy} e^{-K} \Phi_F(x,y)$$

where all dependence on field A_μ is in

$$\Phi_F(x,y) = (P \exp ig \int_y^x A_\mu dz_\mu)(P \exp g \int_0^s d\tau \sigma_{\mu\nu} F_{\mu\nu}) \equiv \Phi\Sigma$$

Φ charge factor, Σ spin factor.

Green's function for $q\bar{q}$ (mesons) or gg (glueballs)

$G_M, G_{Gl} = \int \int$ integral measure $\langle W_\sigma \rangle$

Thus all dynamics is defined by the Wilson loop (with spin factor insertions).

Wilson loop with spin factors

$\langle trW_\sigma(C)\rangle = \exp(-\sigma Area)$ (spin factors)

$$Area = \int_0^T dt \int_0^1 d\beta \sqrt{\dot{w}^2 w'^2 - (\dot{w}w')^2};$$

Note: no DOF on the area after vacuum averaging. Minimal area $\rightarrow$ minimal strings without DOF except at the ends.

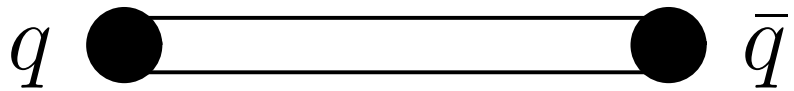

Figure 6:

Hamiltonian of minimal strings with quarks (gluons) at the ends

Last step: from path integral to Hamiltonian

$$G_{q\bar{q}}(x,y) = \langle x| \exp(-HT)|y\rangle \tag{15}$$

For equal current masses $m_q = m_{\bar{q}} = m, \quad \mu_1 = \mu_2 = \mu$

$$H_0 = \frac{m^2 + \mathbf{p}^2}{\mu} + \mu + \frac{\hat{L}^2/r^2}{\mu + 2\int_0^1 d\beta(\beta - \frac{1}{2})^2\nu(\beta)} +$$

$$+\frac{\sigma^2 r^2}{2}\int_0^1 \frac{d\beta}{\nu(\beta)} + \int_0^1 \frac{\nu(\beta)}{2}d\beta. \tag{16}$$

$$\frac{\partial H_0}{\partial \mu_i}|_{\mu_i=\mu_i^{(0)}} = 0, \quad \frac{\partial H_0}{\partial \nu}|_{\nu=\nu^{(0)}} = 0. \tag{17}$$

$\mu_i^{(0)}$ play role of constituent mass of particle i, $\mu_i^{(0)} = \langle\sqrt{m_i^2 + \mathbf{p}^2}\rangle$

$$H_0(L=0) = \sum_{i=1}^{2}\sqrt{m_i^2 + \mathbf{p}^2} + \sigma r. \tag{18}$$

For large $L, L \to \infty$ one obtains a free bosonic string.

$$H_0^2 \approx 2\pi\sigma\sqrt{L(L+1)}, \quad \nu^{(0)}(\beta) = \sqrt{\frac{8\sigma L}{\pi}}\frac{1}{\sqrt{1-4(\beta-\frac{1}{2})^2}}. \tag{19}$$

Constituent masses $\mu_i^{(0)}$ are calculated through σ and m_i.

For quarks, $m=0 \;\; \mu_q = c_n\sqrt{\sigma} = 0.34$ GeV(ground state).

For gluons $\mu_g = \sqrt{C_2}\mu_q = \frac{3}{2}\mu_q = 0.5$ GeV. (Note: This mass is not connected with IR freezing of α_s.)

Total Hamiltonian

$$H = H_0 + H_{self} + H_{spin} + H_{Coul} + H_{rad} + H_{mix}. \tag{20}$$

For H_0 only, $m = 0$

$$M_0^2 \approx 8\sigma L + 4\pi\sigma\left(n + \frac{3}{4}\right), \quad n = 0, 1, 2, ...$$

The input is minimal:

1. Quark current masses m_1, m_2 (pole masses if H_{pert} is used).
2. String tension σ.
3. Background strong coupling $\alpha_B(r)$.

In momentum space in one loop appr.

$$\alpha_B^{(1)}(Q) = \frac{4\pi}{\beta_0} \frac{1}{\ln \frac{(M_0^2+Q^2)}{\Lambda_{QCD}^2}}$$

To be derived later.

Resulting spectra of light mesons are shown.

Orbital excitations (Regge trajectories) vs experiment (Badalian, Bakker).

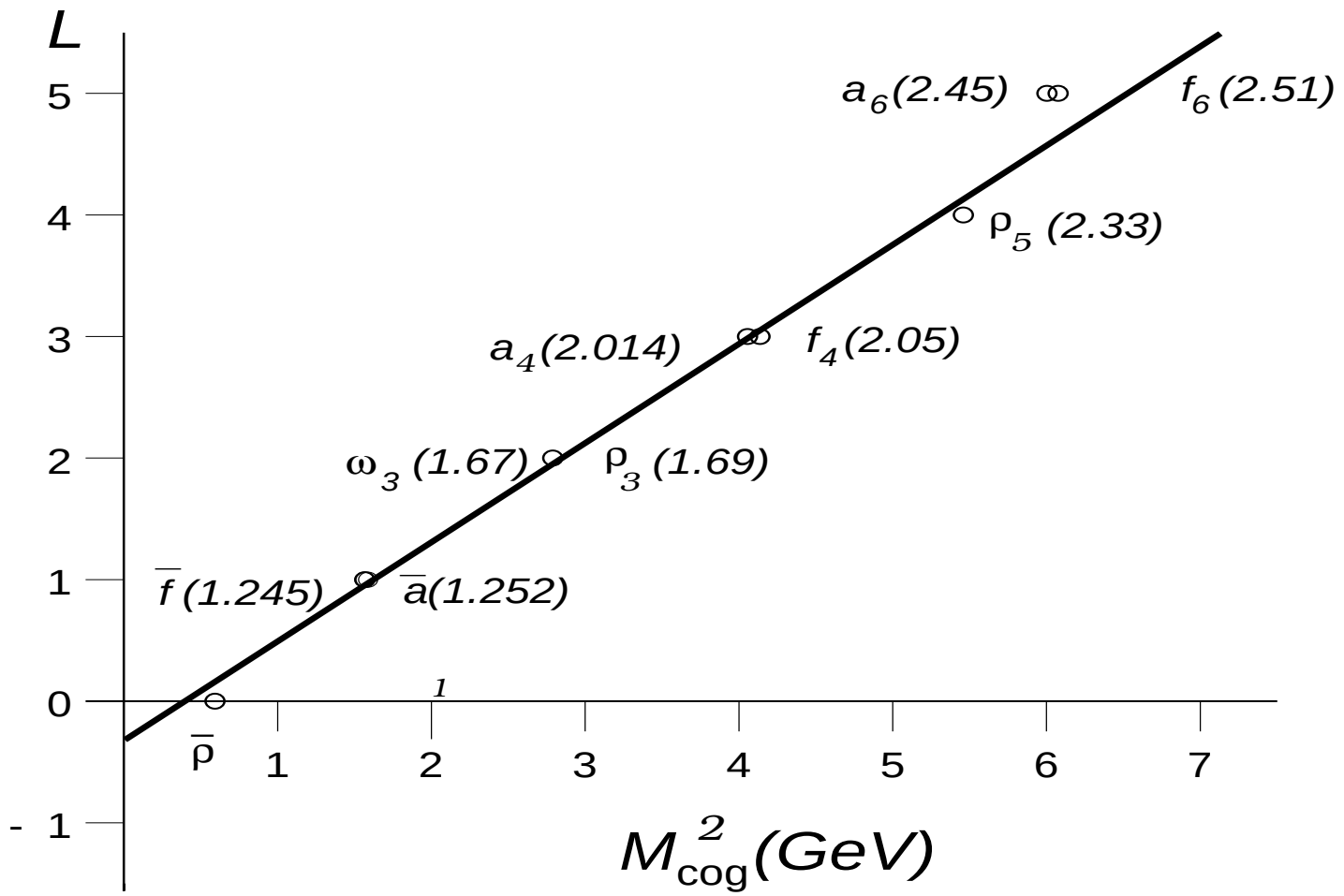

Figure 7: The Regge L-trajectory for the light mesons.

Table 2

Comparison of calculated glueball masses (in GeV) with lattice data ($\sigma_f = 0.18$ GeV^2, $\alpha_s = 0.3$ ($\alpha_s = 0.2$ in parentheses))

J^{PC}	M_{theory} this work	M_{lat} [22]	[23]	[24]
0^{++}	(1.61) 1.41	1.53±0.10	1.53±0.04	1.52±0.13
2^{++}	(2.21) 2.30	2.13±0.12	2.20±0.07	2.12±0.15
0^{++*}	(2.72) 2.41	2.38±0.25	2.79±0.09	
2^{++*}	(3.13) 3.32	2.93±0.14	2.85±0.28	
0^{-+}	2.28	2.30±0.15	2.11±0.24	2.27±0.15
0^{-+*}	3.35	3.24±0.2		
2^{-+}	2.70	2.76±0.16	3.0±0.28	2.70±0.19
2^{-+*}	3.73	3.46±0.21		

Glueballs: Kaidalov+Yu.S.('00,'05).

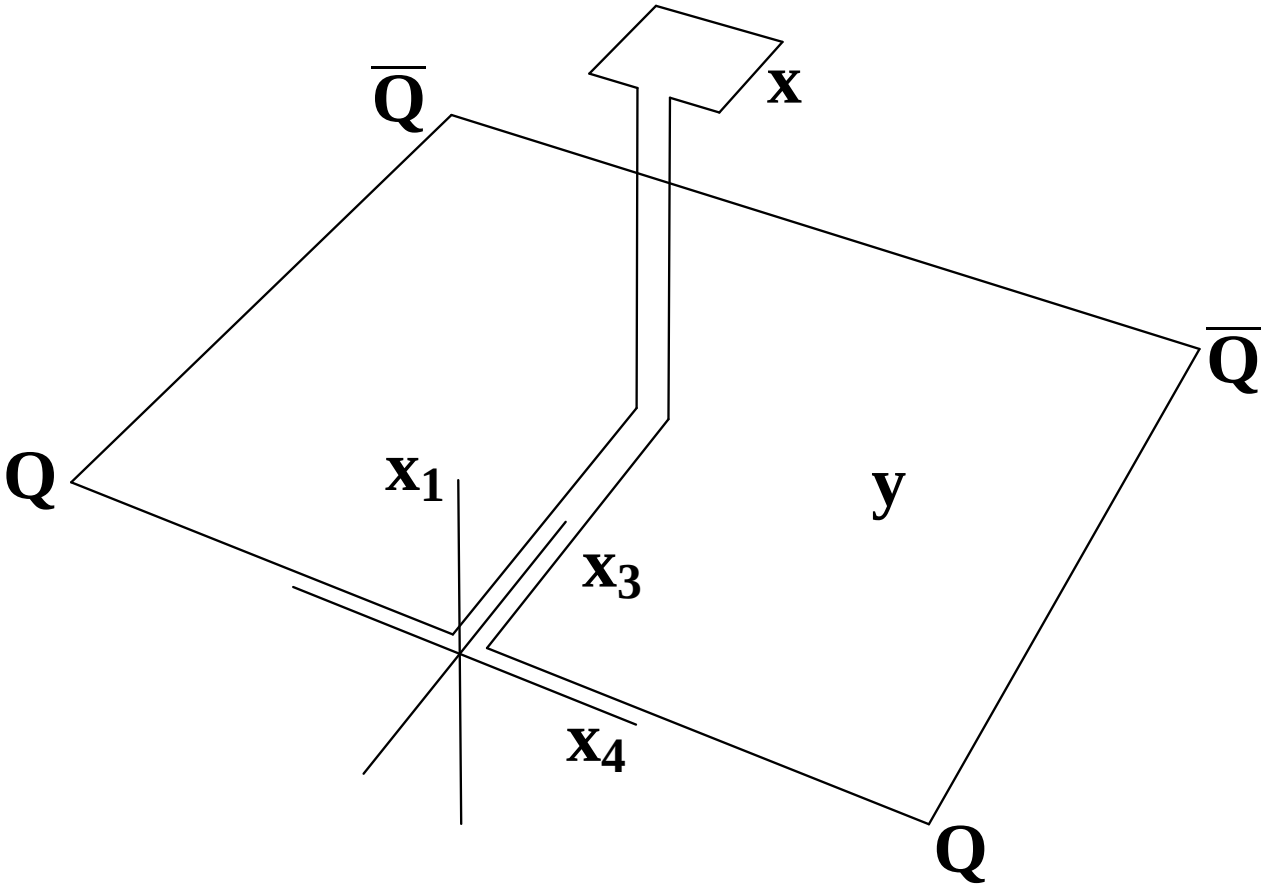

Figure 8: A connected probe for static quark and antiquark

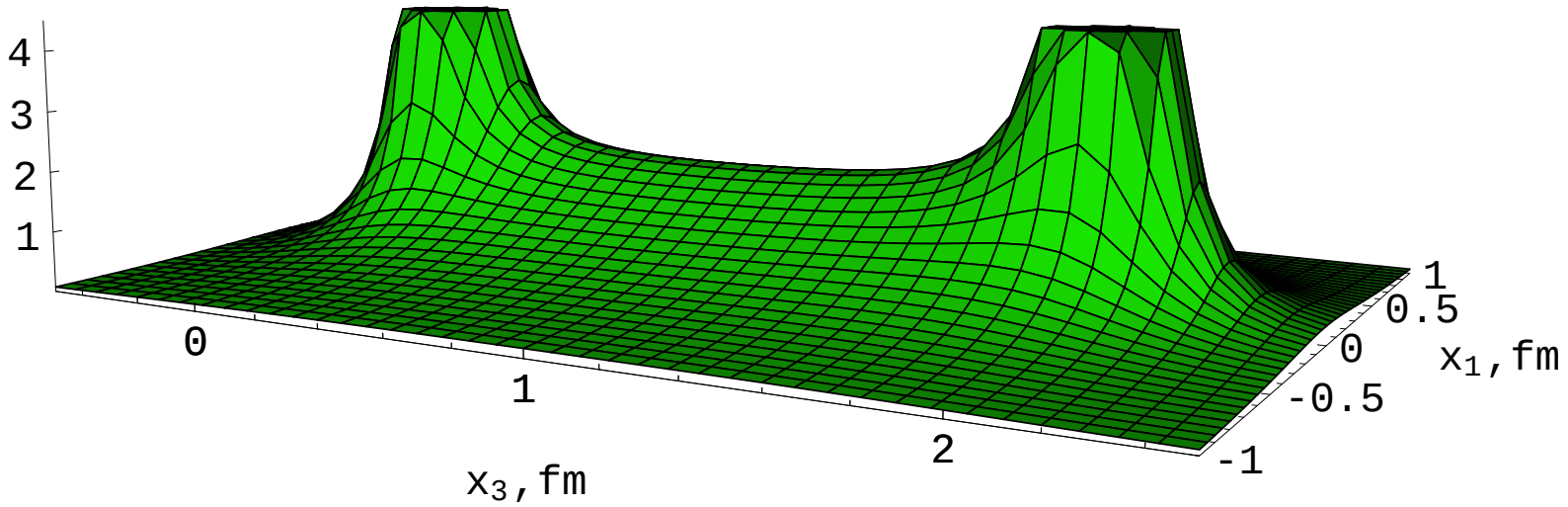

Figure 9: A distribution of the field $|\boldsymbol{\mathcal{E}}(x_1, 0, x_3)|$ at quark-antiquark separation 2 fm. Cutted peaks of color-Coulomb field and string between quark and antiquark are clearly distinguished. The standard values of parameters $\sigma = 0.18$ GeV^2, $\lambda = 0.2$ fm are used.

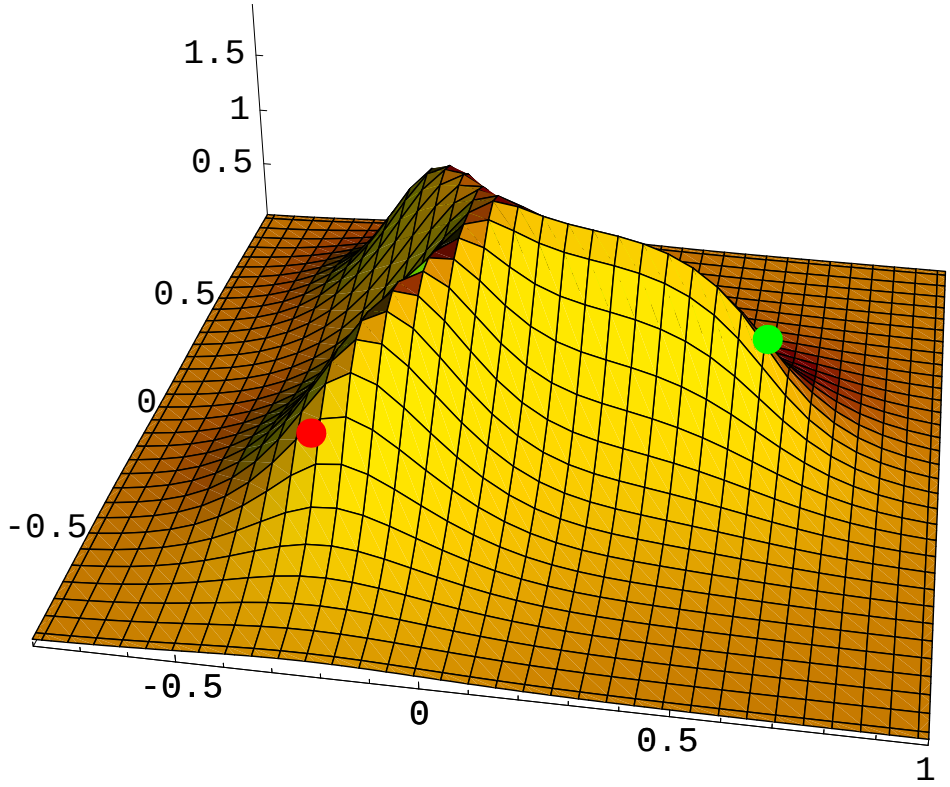

Figure 10: A distribution of the field $\boldsymbol{\mathcal{E}}^{(B)}$ in GeV/fm with the only correlator D contribution considered in the quark plane for equilateral triangle with the side 1 fm. Coordinates are given in fm, positions of quarks are marked by points.

The Y-type string is clearly seen.

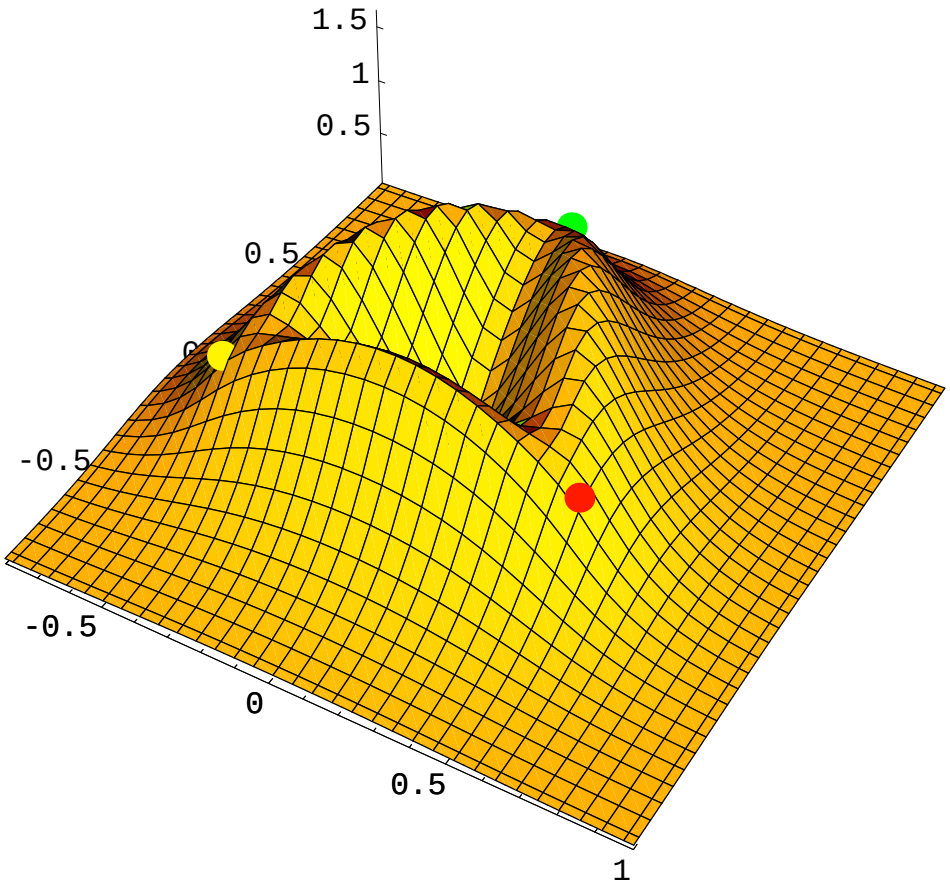

Figure 11: A distribution of the field $|\boldsymbol{\mathcal{E}}_{\Delta}^{(G)}(\mathbf{x})|$ in GeV/fm of the triangular glueball in the plane of valence gluons with separations 1 fm. Coordinates are given in fm, positions of valence gluons are marked by points.

Explaining T_c via gluonic condensate

$$SVZ \quad \varepsilon_{vac} = 1/4\theta_{\mu\mu} = \frac{\beta(\alpha_s)}{16\alpha_s}\langle (F^a_{\mu\nu})^2\rangle \cong -\frac{(11-\frac{2}{3}n_f)}{32}G_2^{(n_f)} \tag{21}$$

$$G_2(0.02 \pm 0.005)\ GeV^4 \text{ S.Narison}$$
$$G_2(0.01 \pm 0.002)\ GeV^4 \text{ Andreev, Zakharov} \tag{22}$$

$$P_1(T) = |\varepsilon_{vac}| + \frac{\pi^2}{30}T^4 + T\sum_k \frac{(2m_kT)^{3/2}}{8\pi^{3/2}}e^{-m_k/T} \equiv |\varepsilon_{vac}| + T^4\chi_1(T). \tag{23}$$

In the deconfined phase one can assume (later confirmed by lattice) (Yu.S. JETP Lett.'92), that

$$D^E(x) = 0 = \sigma_E; \quad D^H(x), D_1^H, D_1^E \neq 0. \tag{24}$$

$$P_2(T) = |\varepsilon_{vac}^{dec}| + T^4(p_{gl} + p_q) \tag{25}$$

Critical line $T_c(\mu)$

$$P_I = |\varepsilon_{vac}| + \chi_1(T) \to \frac{11}{32} G_2$$

$$P_{II} = \frac{11}{32} G_2^{dec} + (p_{gl} + p_q) T^4;$$

$$P_I(T_c) = P_{II}(T_c)$$

$$T_c(\mu) = \left(\frac{\frac{11}{32} \Delta G_2}{p_{gl} + p_q} \right)^{1/4},$$

within 10% $\Delta G_2 \approx \frac{1}{2} G_2$.

$\frac{\Delta G_2}{0.01\ \mathrm{GeV}^4}$	0.191	0.341	0.57	1
$T_c(\ \mathrm{GeV})\quad n_f = 0$	0.246	0.273	0.298	0.328
$T_c(\ \mathrm{GeV})\quad n_f = 2$	0.168	0.19	0.21	0.236
$T_c(\ \mathrm{GeV})\quad n_f = 3$	0.154	0.172	0.191	0.214
$\mu_c(\ \mathrm{GeV})\quad n_f = 2$	0.576	0.626	0.68	0.742
$\mu_c(\ \mathrm{GeV})\quad n_f = 3$	0.539	0.581	0.629	0.686

Field correlators via gluelumps

In this section we calculate D, D_1 analytically via gluelump Green's functions. Physical idea: Nonabelian mean field approach yields confining background field B_μ, with a_μ^a -quanta of gluonic field – propagating in vacuum with a fixed color index a, while $B_\mu \sim A_\mu^b$, $b \neq a$.

$$A_\mu = B_\mu + a_\mu$$

When averaging over B_μ one obtains confining string for a_μ^a.

As a result (Yu.S. '05, Antonov '05) to the lowest order in α_s

$$D_1(x) = -\frac{2g^2}{N_c^2}\frac{dG^{(1)}(x)}{dx^2}$$

$$D(x) = \frac{g^4(N_c^2-1)}{2}G^{(2)}(x)$$

and $G^{(1)}(x)$ is the one-gluon gluelump Green's function, $G^{(2)}$ - the same for two gluons.

For one-gluon-gluelump Green's function $G^{(1)}$ one can write.

$$G^{ab}_{\mu\nu}(x,y) = \left\{ \int_0^\infty ds (Dz)_{xy} e^{-K} P_a \exp(ig \int_y^x \hat{A}_\mu dz_\mu) P_\Sigma(x,y,s) \right\}^{ab}_{\mu\nu}, \tag{26}$$

where

$$P_\Sigma(x,y,s) = P_F \exp(2ig \int_0^s \hat{F}_{\lambda\sigma}(z(\tau)) d\tau).$$

For two-gluon-gluelump $G^{(2)} \sim \langle tr(G^{ab}_{\mu\nu} G^{ba}_{\mu\nu}) \rangle$.

As was shown in [V.Shevchenko, Yu.S., PLB 437 (1998) 146] perturbative terms cancel in $D(x)$ and not in $D_1(x)$.

$$D(z) = D^{np}(z) \;\; ; \;\; D_1(z) = D_1^p(z) + D_1^{np}(z) \tag{27}$$

and general asymptotics for $D_1(z)$ is

$$D_1(z) = \frac{c}{z^4} + \frac{a_2}{z^2} + O(z^0). \tag{28}$$

Finally, for G_2

$$G_2 = \frac{6N_c}{\pi^2}(D^{np}(0) + D_1^{np}(0)) \tag{29}$$

For $G^{(1)}$ and $G^{(2)}$ one has path integrals

$$G_{\mu\nu}^{(1gl)}(x,y) = \mathrm{Tr}_a \int_0^\infty ds (Dz)_{xy} \exp(-K) \langle W_{\mu\nu}^F(C_{xy}) \rangle, \tag{30}$$

$$G^{(2gl)}(z) = \int_0^\infty ds_1 \int_0^\infty ds_2 (Dz_1)_{0x} (Dz_2)_{0x} \mathrm{Tr} W_\Sigma(C_1, C_2). \tag{31}$$

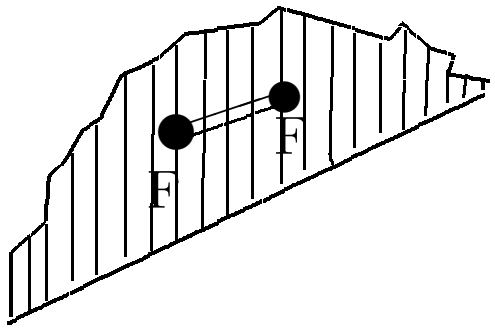

Fig. 13 One-gluon gluelump for $D_1(x)$

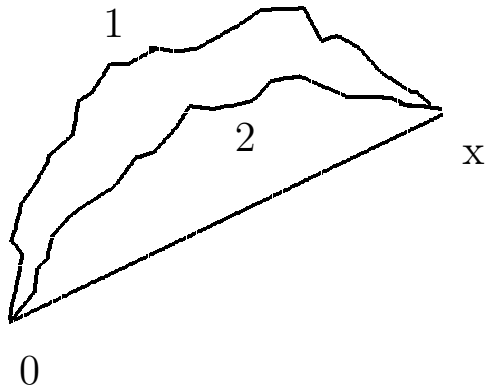

Fig. 15 Two-gluon gluelump for $D(x)$

Using Hamiltonian formalism for gluelumps, one has asymptotics,

$$D(x) \sim \exp\left(-|x|/\lambda\right), \quad D_1(x) \sim \exp\left(-|x|/\lambda_1\right)$$
$$\lambda = \frac{1}{M_0^{(2)}}, \quad \lambda_1 = \frac{1}{M_0^{(1)}},$$

where $M_0^{(2)}$ –lowest 2g gluelump mass,

$M_0^{(1)}$ – lowest 1g gluelump mass.

Specifically

$$D_1(z) = \frac{2C_2(f)\alpha_s M_0^{(1)}\sigma_{adj}}{|z|} e^{-M_0^{(1)}|z|}, \quad |z|M_0^{(1)} \gg 1. \tag{32}$$

where $M_0^{(1)} = (1.2 \div 1.4)$ GeV for $\sigma_f = 0.18$ GeV^2 [**?**, **?**].

$$D(z) = \frac{g^4(N_c^2-1)}{2} 0.1\sigma_f^2 e^{-M_0^{(2)}|z|}, \quad M_0^{(2)}|z| \gg 1 \tag{33}$$

where $M_0^{(2)} = (2.5 \div 2.6)$ GeV.

Table

Comparison of gluelump masses from lattice (C.Michael, Foster) and string Hamiltonian (Yu.S. '00)

J^{PC}	1^{+-}	1^{--}	2^{--}	2^{+-}	3^{+-}	0^{++}
M (GeV) lattice	1.87	2.23	2.45	2.84	2.84	2.96
M (GeV) QCD string	1.87	2.34	2.36	2.70	2.71	2.78

Thus $M_0^{(1)}$ and $M_0^{(2)}$ are expressed solely via $\sqrt{\sigma}$:

$$M_0^{(i)} = c_i\sqrt{\sigma}, \quad c_1 \cong 3, \quad c_2 \cong 5$$

and the corresponding vacuum correlation lengths $\lambda^{(1)}, \lambda^{(2)}$ of $D_1(x), D(x)$ are also connected to $\sqrt{\sigma}$:

$$\lambda^{(1)} = \frac{1}{c_1\sqrt{\sigma}}, \quad \lambda^{(2)} = \frac{1}{c_2\sqrt{\sigma}}, \quad \lambda^{(2)} \equiv \lambda.$$

We now understand why λ is so small

$$\lambda \approx 0.1 fm$$

9. Check of selfconsistency

Since np parts of $D(x), D_1(x)$ are calculated in $G^{(1)}, G^{(2)}$ through correlator $\langle F(x)F(y)\rangle$, i.e. via $D(x), D_1(x)$, one should check selfconsistency.

At small distances: there are corrections to $D_1(x)$ from diagrams

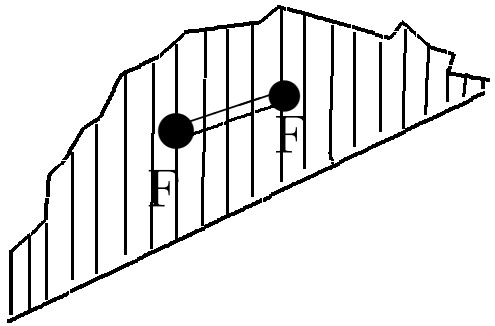

Fig. 16

Leading correction at small x comes from this diagram, where Wilson loop at small x (and small area S) has the limit (Dosch and Yu.S.'87)

$$\langle W \rangle \cong \exp\left(-\frac{\pi^2}{8} G_2 S^2\right)$$

which yields for $D_1(x)$

$$D_1(z) = \frac{4C_2(f)\alpha_s}{\pi}\frac{1}{z^4} + \frac{g^2}{12}G_2. \tag{34}$$

It is remarkable that the sign of the *np* correction is positive.

For $D(z)$ situation is more complicated. Leading np corrections at small z come from two diagrams, Fig. 18 and Fig. 19.

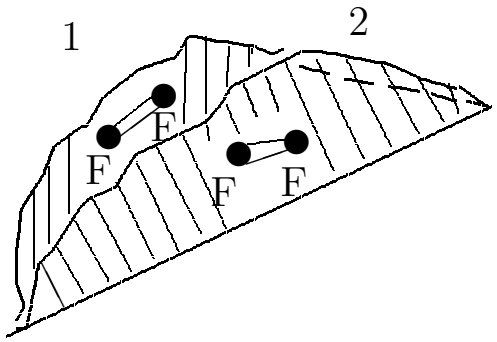

Fig. 18

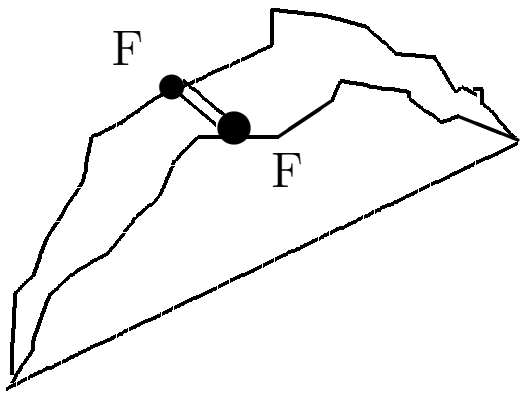

Fig. 19

These diagrams yield at small z np corrections

$$D(z) \approx -4N_c\alpha_s^2(\mu(z))G_2 + N_c^2\frac{\alpha_s^2(\mu(z))}{2\pi^2}D(\lambda_0)\log^2\left(\frac{\lambda_0\sqrt{e}}{z}\right) \quad (35)$$

But at small z $\alpha_s(\mu(z)) \sim 2\pi/\beta_0 log(\Lambda z)^{-1}$, the first term is subleading, and second tends to a constant (which means constant gluonic condensate!)

$$D(0) = \frac{N_c^2}{2\pi^2}D(\lambda_0)\left(\frac{2\pi}{\beta_0}\right)^2 \quad (36)$$

Here λ_0 is near maximum of $D(z)$, $\lambda_0 \gtrsim \lambda$, and for $N_c = 3$ one obtains $D(0) \approx 0.15D(\lambda_0)$. As a result one has behaviour of $D(z)$ shown in the Fig. 20.

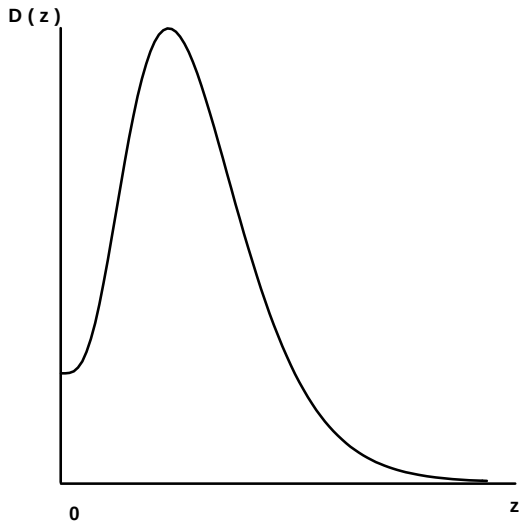

Fig. 20. Semiquantitative behavior of the correlator $D(x)$ at all distances

This pattern may solve qualitatively the contradiction between the values of $D(0)$ estimated from the string tension $D_\sigma(0) \simeq \frac{\sigma}{\pi\lambda^2} \approx 0.35$ GeV^4 and the value obtained in naive way from the gluon condensate $D_{G_2}(0) = \frac{\pi^2}{18} G_2 \approx (0.007 \div 0.012)$ GeV^4. One can see that $D_\sigma(0) \approx (30 \div 54) D_{G_2}(0)$. This seems to be a reasonable explanation of the mismatch discussed in the introduction. This explains why G_2 is so small.

Now we shall show that in our approach of gluelumps as field correlators one can establish connection between perturbative scale Λ_{QCD} and nonperturbative scale, say, σ. Using asymptotics of gluelump Green's function one can write the large distance behaviour of $D(z)$ as

$$D(z) \equiv D_\sigma(0) \exp(-M_0^{(2)}|z|), \quad D_\sigma(0) = g^4 \frac{(N_c^2-1)}{2} 0.1 \sigma_f^2. \qquad (37)$$

On the other hand, from (32) one has integrating $D(z)$ (and taking into account that at small $z, D(z)$ is smaller than (37), see Fig.).

$$\sigma = \frac{1}{2}\int D(z)d^2z \leq \frac{\pi D_\sigma(0)}{(M_0^{(2)})^2} = 0.17\pi^3\alpha_s^2(\mu)\frac{(N_c^2-1)\sigma_f^2}{(M_0^{(2)})^2} \qquad (38)$$

Here μ corresponds to the average momentum (inverse radius) of the two-gluon gluelump with mass $M_0^{(2)}$. The latter was computed in terms of σ_f, $M_0^{(2)} \cong 5.6\sqrt{\sigma_f}$, and one has from (83)

$$\alpha_s^2(\mu) \geq 0.16, \quad \mu = \sqrt{\langle k_{gl}^2\rangle} \approx 2\sqrt{\sigma_f}.$$

Or to the lowest order $\Lambda_{QCD} \geq 0.17\mu = 0.16$ GeV.

This is in the correct ballpark, since realistic Λ_{QCD} in $\overline{MS}$ scheme for $n_f = 2$ is around 0.25 GeV, however for better accuracy one needs to take into account NLO terms and nonasymptotic behaviour of $D(z)$ at small z, which will increase estimate of Λ_{QCD}.
On general grounds, one may preview, that any connection of Λ_{QCD} with np scale will have the form: $\alpha_s(\mu_{np}) = C$, where μ_{np} is defined by np effects and scale, and C is a fixed number.
Thus we have a consistency check for $D(x), D_1(x)$ both at small and large distances.

10. Conclusions

1. Field correlator Method provides the explicit dynamical theory for Large-Distance QCD. The confinement is due to nonperturbative correlators of colorelectric fields, and for a flat (minimal) surface the lowest Gaussian correlator $D^E(x)$ plays the dominant role. Cluster expansion in n-th order correlators behaves as $\sim (\sigma\lambda^2)^n = (0.05)^n$.
2. Correlation length λ and correlators are calculated selfconsistently via gluelumps, $\lambda_D^E \approx 0.1$ fm. Thus one has a theory defined by the only parameter say σ (in addition to current quark masses).
3. The leading pert. and np terms enter additively at small distances in field correlators and selfconsistency is maintained both at small and large distances. In particular, Λ_{QCD} is connected to σ.
4. Within our method one can explain quantitatively all the mass scales in QCD.